J Mol Model (2015) 21: 266
DOI 10.1007/s00894-015-2818-7

ORIGINAL PAPER

On the correction of calculated vibrational frequencies for the effects of the counterions — α,ω-diamine dihydrochlorides

S. M. Fiuza[1] · T. M. Silva[1] · M. P. M. Marques[1,2] · L. A. E. Batista de Carvalho[1] · A. M. Amado[1]

Received: 29 July 2015 / Accepted: 7 September 2015 / Published online: 19 September 2015

Abstract The present work provides sets of correction factors to adjust the calculated vibrational frequencies of a series of α,ω-diamines hydrochloride salts to account for the intermolecular interactions with the counterion. The study was performed using different theory levels for predicting the vibrational data of isolated dicationic α,ω-diamines and their hydrochloride forms, with and without the explicit account of the interactions with the chloride counterions. Different sets of correction factors were determined for each theory level considering the four smallest elements for the α,ω-diamines series, while their transferability and reliability was evaluated considering the larger elements of the series. The theory level simplification was also evaluated and was found to neither compromise the vibrational frequencies estimates nor the magnitude and accuracy of the pre-defined scaling factors. This suggests that transferability of the correction factors is possible not only for different diamines but also between different levels of theory with the averaged group correction factor, ζ_g^a, being the best choice to account for the effects of the N–H···Cl interactions. The possibility of simplifying the theory level without compromising efficiency and accuracy is additionally of utmost importance. This computational approach can constitute a valuable tool in the future for studying the hydrochloride forms of larger and more complex diamine systems.

Keywords Aliphatic diamines · Counterion effect · Quantum chemical calculations · Vibrational frequencies

Introduction

Polyamines are ubiquitous molecules in living organisms. They have attracted a great interest over the years because of their multiple and vital functions in cell biology and biochemistry [1–13]. Their polycationic character at physiological pH renders them able to interact and/or bind with various important cellular macromolecules, including DNA, RNA and proteins, thereby affecting their activity [4, 5, 7, 9, 11, 14–16]. Numerous recent studies have shown that alkylpolyamines can act as ligands to metal ions such as Pt (II) and Pd (II), and that some of the resulting complexes display promising anticancer properties [17–23].

In the last few years, the authors have been involved in a project aimed at understanding the structure-activity relationships (SARs) underlying the anticancer properties of some Pt(II)– and Pd(II)–polyamine complexes. Characterization of both free ligands and metal complexes has been performed by vibrational spectroscopy (Raman, Fourier transform infrared (FTIR) and inelastic neutron scattering (INS)) coupled to quantum chemical calculations [24–34].

Quantum chemical calculations are frequently performed for the isolated molecule. This simplification, however, may compromise the calculations accuracy since it completely neglects the effects of the intermolecular interactions occurring in the condensed phase. In a previous quantum chemical study performed for the 1,2-ethylenediamine dihydrochloride salt

Electronic supplementary material The online version of this article (doi:10.1007/s00894-015-2818-7) contains supplementary material, which is available to authorized users.

✉ A. M. Amado
amado.am@gmail.com

[1] I&D Unit "Química-Física Molecular", Department of Chemistry, Faculty of Science and Technology, University of Coimbra, P-3004-535 Coimbra, Portugal

[2] Department of Life Sciences, University of Coimbra, 3000-456 Coimbra, Portugal

[26], for instance, the authors verified that accounting for the interactions between the protonated amine groups and the surrounding chloride counterions is essential for an accurate prediction of the corresponding vibrational spectra. The explicit consideration of the counterions is, however, associated to significant computational costs that may render calculations unfeasible. Density functional theory with periodic boundary conditions (periodic-DFT) can be used for representing the entire unit cell [30–32] (thus, explicitly including intermolecular interactions). However, once again, the method becomes rapidly inapplicable with increasing system size. Therefore, the definition of a methodology that weighs the effects of intermolecular interactions, without causing a rapid prohibitive enhancement of computational demands, is of the utmost relevance.

The main goal of the present study is to test the possibility of using pre-defined correction factors to correct the vibrational frequencies calculated for the isolated cationic forms of polyamines for the effects of the intermolecular interactions that occur in the condensed phase. The hydrochlorides of the α,ω-diamine series (general formula $[H_3N(CH_2)_nNH_3]^{2+}$, n= 2 – 10 and 12; Fig. 1) were selected to perform the study. The principle of factor transferability for correcting quantum chemical vibrational frequencies for unaccounted effects is not new. In fact, pre-defined scaling factors are widely used to correct the calculated vibrational frequencies for anharmonicity effects and incomplete treatment of electron correlation, which are underestimated by the currently used single-molecule theoretical levels [35–37].

The present study has an additional goal. One of the factors that limits the applicability of quantum chemical calculations to large molecular systems is related to the theory level considered. Thus, this work also intended to infer on the efficiency of the simple mPW1PW/6-31G* theory level relative to a significantly more complex approach ωB97XD/6-311++G(2d,2p). This assessment is important since a proper simplification of the level of theory can contribute to a significant broadening of the applicability of quantum chemical calculations.

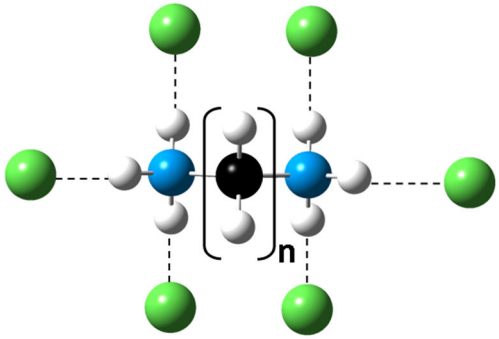

		nomenclature
n = 2	1,2-diaminoethane	DAE
n = 3	1,3-diaminopropane	DAPro
n = 4	1,4-diaminobutane (putrescine)	DAB
n = 5	1,5-diaminopentane (cadaverine)	DAPen
n = 6	1,6-diaminohexane	DAHex
n = 7	1,7-diaminoheptane	DAHep
n = 8	1,8-diaminooctane	DAO
n = 9	1,9-diaminononane	DAN
n = 10	1,10-diaminodecane	DADec
n = 12	1,12-diaminododecane	DADod

Fig. 1 Schematic representation of the α,ω-diamine series considered in this study, along with the nomenclature used throughout the text and Tables

Computational details

Calculations were performed using the Gaussian 09w program (G09w) [38], installed in a PC machine. All calculations were performed considering the mPW1PW DFT combined with the widely used 6-31G* basis set (**mPW1PW/6-31G***), as implemented in G09 [38]. In the case of the four smallest elements of the α,ω-diamines series, calculations were also performed using the long-range corrected hybrid DFT ωB97XD combined with the 6-311++G(2d,2p) basis set (**ωB97XD/6-311++G(2d,2p)**). For simplification, these two theory levels (**TL**) are designated by **TL-1** and **TL-2**, respectively, in Table 1. Other DFT methods (hybrid functionals M06-2X and X3LYP, and the long-range corrected hybrid functionals LC-wPBE) and basis sets (6-31G**, 6-31++G**, and aug-cc-pVDZ) were also tested, but due to the similarity between the overall results, they will not be discussed extensively. Any further information concerning these DFT/basis set combinations can be obtained by request to the authors.

The authors are aware of the smallness and limitations of the 6-31G* basis set used. However, the use of this theory level is justified as the present work integrates a wider project on the study of significantly larger aliphatic amines, as well as of their Pd(II) and Pt(II) complexes. Previous reports on the theoretical prediction of the vibrational spectra of *cis*-diamminedichloro-platinum (II) (cisplatin) and *cis*-diamminedichloro-palladium (II) [25, 28] showed that the mPW1PW/6-31G* theory level yielded a good balance between the computational demands and the accuracy achieved. This theory level has also been demonstrated to be adequate for the description of hydrogen bonds involving N–H groups [24]. Despite these prior findings, the efficiency of the mPW1PW/6-31G * level was once more evaluated, within this new context, by comparison with the results obtained using a higher theory level that combines a long-range

Table 1 Group correction factors (ζ_g) and average group correction factors (ζ_g^a) determined for the mPW1PW/6-31G* and ωB97XD/6-311++G(2d,2p) theory levels [a]

Vibrational mode [b]	ζ_g								ζ_g^a [c]	
	DAE		DAPro		DAB		DAPen			
	TL-1	TL-2	TL-1	TL-2	TL-1	TL-2	TL-1	TL-2	TL-1	TL-2
ν NH_3	0.88	0.89	0.88	0.89	0.88	0.88	0.87	0.88	0.88	0.89
δ NH_3	1.01	1.01	1.01	1.01	1.01	1.01	1.01	1.01	1.01	1.01
ρ NH_3	1.07	1.07	1.06	1.06	1.06	1.06	1.06	1.06	1.06	1.06
τ NH_3	2.43	2.34	2.43	2.32	2.46	2.40	2.51	2.34	2.46	2.35
ν CH_2	1.00	1.00	1.00	1.00	1.00	1.00	1.00	1.00	1.00	1.00
δ CH_2										
ω CH_2										
t CH_2										
ρ CH_2										
ν C–C	0.91	0.91	0.95	0.94	0.98	0.98	0.99	0.98	0.97	0.97
ν C–N	1.13	1.13	1.17	1.17	1.17	1.17	1.19	1.18	1.17	1.16

(a) TL-1=mPW1PW/6-31G* and TL-2=ωB97XD/6-311++G(2d,2p), respectively)

(b) ν=stretching; δ=deformation; t=twisting; ρ=rocking; ω=wagging; τ=torsion

(c) average values of the corresponding ζ_g -values obtained for the four α,ω-diamines

corrected hybrid functional, ωB97XD, with a much larger basis set, 6-311++G(2d,2p). The choice of this theory level was based on its well documented high performance regarding the description of hydrogen bonding [39–42].

Assembling of the starting geometries

For each linear α,ω-diamine (Fig. 1), full geometry optimization and vibrational frequency calculations were performed considering the isolated dicationic amine (i.e., neglecting the presence of the counterions) and the corresponding hydrochloride form. Throughout the text and tables, the distinction between the two forms is made by appending a suffix, either **–H** (dicationic) and **–HCl** (hydrochloride), to the acronym used to identify the diamine (Fig. 1).

Assembly of the starting geometries for different hydrochloride adducts was performed using the X-ray information available in the literature [43–53] and the theoretical results previously reported for DAE-HCl [26]. Briefly, in all cases, the diamine cation skeleton presents an almost all-*trans* configuration, with both NH_3^+-terminals involved in three strong N–H···Cl hydrogen bonds to distinct surrounding counterions. In turn, each counterion establishes contacts with three distinct neighboring diamine cations. This relative spatial arrangement of the diamines and counterions gives rise to two-dimensional layers, which are stacked one onto the other by additional weaker N–H···Cl and C–H···Cl intermolecular interactions. Despite this complex overall arrangement, the quantum chemical results obtained for DAE-HCl [26] showed that an overall arrangement presenting one diamine cation surrounded by six counterions (Fig. 1) constitutes a good model for predicting the vibrational frequencies of DAE within the crystal packing.

Determination of the correction factors and transferability evaluation

Determination of the correction factors was performed considering only the four shortest diamines of the α,ω-diamine series (DAE, DAPro, DAB, and DAPen). The remaining elements of the series were included in the evaluation of the transferability of the correction factors, performed subsequently.

The appropriate match between the vibrational frequencies predicted (ω_i) for both the dicationic and hydrochloride forms of DAE, DAPro, DAB, and DAPen was performed by visualizing the atomic displacements characterizing each vibrational mode using the GaussView program [54]. In the case of the NH_3 antisymmetric stretching ($\nu_{as}NH_3$), antisymmetric deformation ($\delta_{as}NH_3$) and rocking (ρNH_3) modes, the correlation between different calculations requires a careful inspection of the atomic displacements involved, as evidenced in Fig. 2. Subsequently, the deviation predicted for each vibrational mode, due to the interaction with the counterions, was determined as

$$\Delta_i = \omega_i(\text{amine}-\text{HCl}) - \omega_i(\text{amine}-\text{H}) \quad (1)$$

An individual correction factor (ζ_i) was determined for each vibrational mode according to the formula:

$$\zeta_i = \frac{\omega_i(\text{amine}-\text{HCl})}{\omega_i(\text{amine}-\text{H})} \quad (2)$$

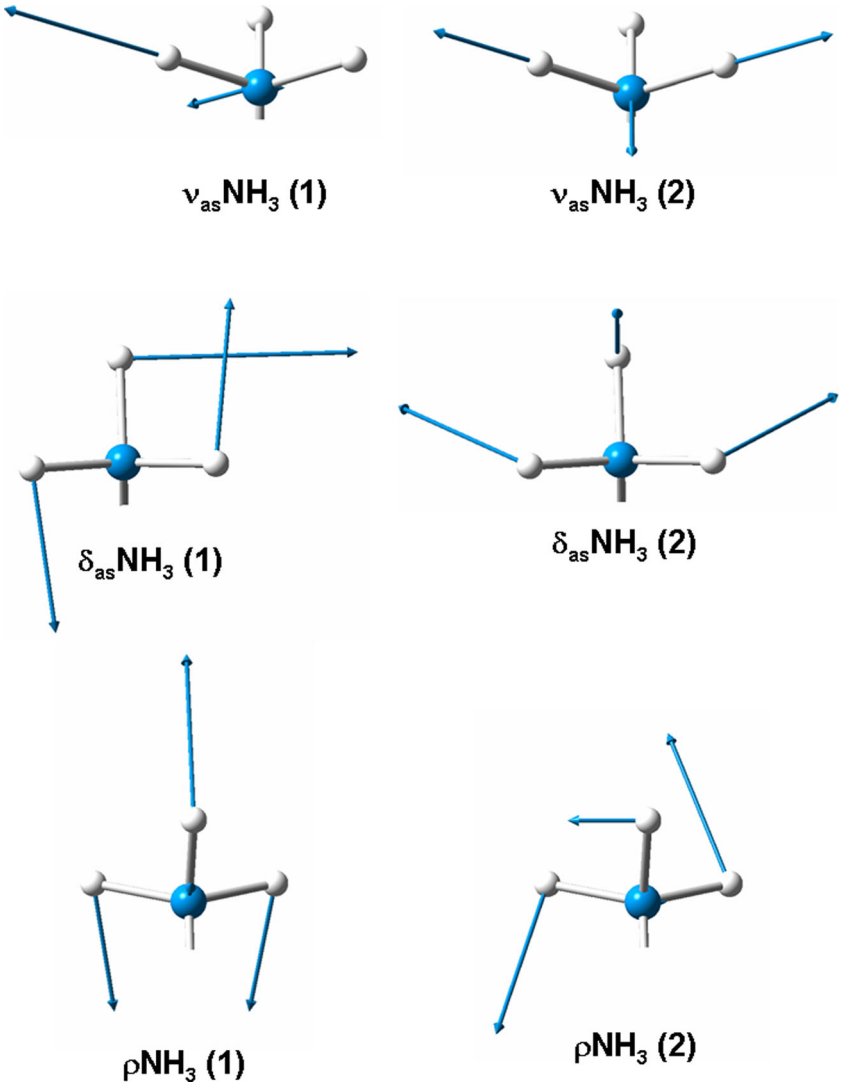

Fig. 2 Schematic representation of the distinct atomic displacements that characterize the rocking, antisymmetric stretching, and deformation modes of the NH_3^+-groups

The similarities found in the magnitude for some ζ_i-factors allowed, at first glance, to define a set of group correction factors (ζ_g) that can be used to correct groups of vibrational modes. Finally, the obtained sets of individual and group correction factors obtained (four sets of each) were used to obtain the corresponding averaged individual and group correction factors ζ_i^a or ζ_g^a, respectively. These were then used to evaluate the transferability of the correction factors among the whole α,ω-diamine series.

At this stage, it is important to refer that the present work did not focus on the longitudinal (βNCC and βCCC) and transversal (γNCC and γCCC) skeletal deformation modes (commonly known as LAMs and TAMs, respectively). These low-frequency acoustic modes constitute a special group of vibrations that are strongly dependent on both length and even/odd character of the carbon skeleton chain [27, 55, 56]. Such behavior discards the possibility of correction factors transferability among systems of different chain size in what concerns the LAM and TAM modes.

Evaluation of the correction method efficiency

The efficiency of the proposed correction methodology of the vibrational frequencies for the effects of the counterions was quantitatively assessed using two statistical parameters, namely the root-mean-square deviation (RMSD) and the coefficient of variation of the root-mean-square (CV; %). These two parameters were determined, respectively, as:

$$\mathrm{RMSD} = \frac{\sqrt{\sum_{i=1}^{n} \left[\zeta \times \omega_i(\text{amine–H}) - \omega_i(\text{amine–HCl})\right]^2}}{n} \quad (3)$$

$$\mathrm{CV} = \frac{\mathrm{RMSD}}{\mu} \times 100 \quad (4)$$

where ζ stands either for the average ζ_i^a or ζ_g^a values, and **n** stands for the number of vibrational modes of the dicationic diamine considered in the analysis (given as **3N-6-L-T**, where

N stands for the number of atoms and L and T stand for the number of LAM and TAM modes, respectively). The μ-value corresponds to the average of the vibrational frequencies calculated for the given diamine–HCl species. Regarding the RMSD values associated to the uncorrected results (**UC**), a ζ-value of 1.00 is assumed for all vibrational modes.

Results and discussion

Effect of simplifying the theory level

The ratio between accuracy and computational demand is undoubtedly one issue of particular relevance in quantum chemical studies. Although it is essential to ensure a high reliability of the computational predictions, keeping the computational demand low is also a fundamental issue in order to broaden the applicability of quantum chemical calculations. Hence the importance of evaluating the efficiency of a relatively simple theory level relative to a much higher one, which in theory provides better predictions but will have a much more restricted applicability due to higher computational requirements.

In order to proceed to the accuracy evaluation of the mPW1PW/6-31G* theory level, the first step consisted of the assessment and comparison of the frequency values provided by both theory levels for the different vibrational modes of DAE, DAPro, DAB, and DAPen, in both dicationic forms (isolated and hydrochloride). Table S1 (Supplementary material) presents the full list of the calculated vibrational frequencies, as a function of diamine, together with the deviations observed due to theory level simplification (in each case, $\Delta=\omega_i$(mPW1PW/6-31G* – ω_i(B97XD/6-311++G(2d,2p)).

Regardless of the diamine size, most of the absolute Δ-values are well below the threshold of 25 cm^{-1}. The most affected vibrational modes partly depend on the dicationic form considered. In the case of the isolated dicationic form, the most affected are the CH_2 symmetric and antisymmetric stretching modes (ν_sCH_2 and $\nu_{as}CH_2$, respectively), the NH_3 symmetric stretching mode (ν_sNH_3) and the NH_3 symmetric and antisymmetric deformation modes (δ_sNH_3 and $\delta_{as}NH_3$, respectively). On the other hand, when an explicit account is given to the N–H···Cl interactions the list of the most affected modes is enlarged to encompass as well the CH_2 deformation modes (δCH_2), the NH_3 antisymmetric stretching ($\nu_{as}NH_3$), and the torsional (τNH_3) modes. Independent of the cationic form considered, it is found that, relative to the ωB97XD/6-311++G(2d,2p) calculations, the mPW1PW/6-31G* theory level tends to underestimate the νNH_3 and the νCH_2 modes and to overestimate the remaining ones.

Figure 3 shows the variation of the mean absolute deviations values (MAD) as a function of diamine dicationic species, for the vibrational modes displaying higher sensitivity to the change in the theory level (ωB97XD/6-311++G(2d,2p) → mPW1PW/6-31G*). For each diamine, left and right columns refer to the –H and –HCl forms, respectively. Independently of the diamine size, changing theory level has a relatively similar effect on the predicted δNH_3 vibrational frequencies. In addition, the νNH_3 and τNH_3 modes are significantly more affected by the theory level simplification for the hydrochlorides than for the –H species.

The effect on the νCH_2 and δCH_2 vibrational modes is not as straightforward. In the case of DAE up to DAB, the νCH_2 and δCH_2 vibrational modes are found to be slightly more affected in the isolated and hydrochloride cations, respectively. However, further increase of the diamine carbon chain (beyond DAPen) seems to annul this differentiation.

Another effect that needs to be scrutinized relates to the magnitude of the deviations of the vibrational frequencies calculated for dicationic DAE, DAEPro, DAB, and DAPen (Δ_i) as a result of the explicit account of the counterions. Table S2 (Supplementary material) gives the full list of Δ_i-values as a function of diamine and theory level. In line with the results previously obtained for DAE-HCl at the B3LYP/6-31G* theory level [26], it is found that the effects promoted by the interactions with the counterions do not manifest themselves evenly over all vibrational modes. The CH_2-related vibrations are unanimously estimated as nearly insensitive to the establishment of the N–H···Cl interactions. Conversely, the NH_3^+-related modes are significantly affected. Among these, the ν_sNH_3, $\nu_{as}NH_3$, and τNH_3 are the most disturbed, with the νNH_3 and τNH_3 vibrations being downward and upward shifted far beyond 250 cm^{-1}. In turn, the δNH_3 and ρNH_3 are comparatively less perturbed, with the former being almost insensitive to the establishment of the N–H···Cl interactions. Finally, regarding the skeletal stretching modes it is found that the C–N stretchings (νC–N) are significantly more affected than the C–C stretchings (νC–C), probably due to their proximity to the interacting counterions. All these general variation trends stand regardless of the diamine and theory level considered (Table S2).

Figure 4 displays the magnitude variation of the Δ_i-values for some selected vibrational modes, as a function of diamine and theory level. In each set, left and right columns refer to the mPW1PW/6-31G* and ωB97XD/6-311++G(2d,2p) results. Analysis of the figure confirms the similarity of the deviations promoted by the explicit counterion account on the vibrational frequencies predictions within both theory levels. Only in a few cases (e.g., νCH_2 and νNH_3) the differences reach a magnitude beyond 50 cm^{-1} (Fig. 4 and Table S2). Yet, the relevance of these more marked differences is attenuated given that they are generally associated to vibrational modes of high frequency value (>3000 cm^{-1}).

The νC–C modes were considered in Fig. 4, despite the evident low sensitivity to the effects of interactions with counterions, only to highlight that their sensitivity becomes gradually lower as the carbon chain size increases. The same is,

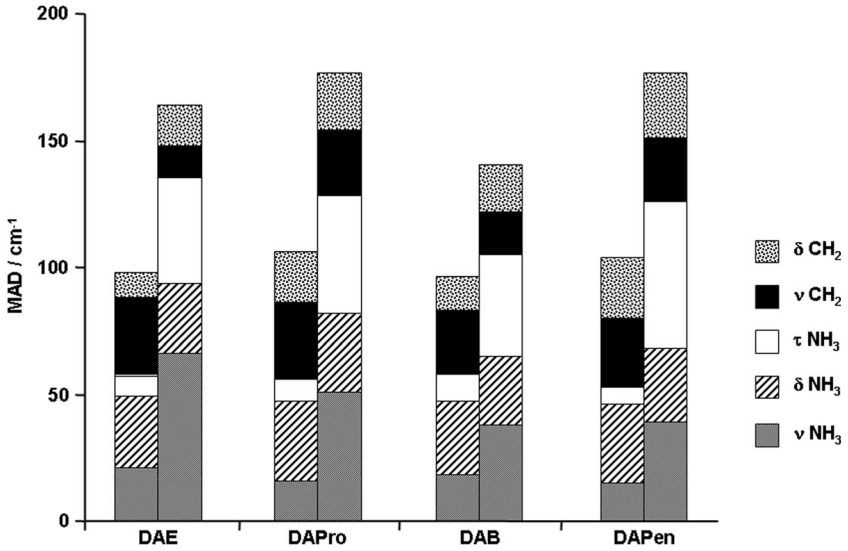

Fig. 3 Variation of the mean absolute deviations (MAD) values for the most affected vibrational modes of DAE, DAPro, DAB, and DAPen, after changing theory level (ωB97XD/6-311++G(2d,2p) to mPW1PW/6-31G*). For each α,ω-diamine, left and right columns refer to the –H and –HCl forms, respectively

however, not observed for the νC–N modes, which demonstrate constancy in the magnitude of the effects promoted, regardless of the diamine and the level of theory. This differential behavior of the νC–N and νC–C modes is probably related to the gradual weakening of the coupling between the two terminal NH_3^+-groups as the carbon chain gets longer. In other words, as the distance between the two NH_3^+-groups increases, the effects of the establishment of the N–H···Cl contacts become gradually more centered on the vibrational modes that directly involve those groups, leaving the νC–C modes progressively out of the effect.

Taken together, the gathered results suggest that the reliability of the effects that are anticipated for the vibrational frequencies of DAE, DAPro, DAB, and DAPen due to explicit account of the N–H···Cl interactions is not compromised by theoretical level simplification. As stated already, one additional parameter that is relevant to scrutinize is the difference between the two levels of theory with respect to their computational requirements. Within the aims of the present work, this evaluation is relevant from different outlooks, namely regarding the gradual increase of the carbon skeleton, the explicit simulation of the presence of the counterions and the theory level simplification. All these evaluations may be based on computational parameters such as the central processing unit (CPU) time required for a frequency calculation and the dimension of the scratch files (e.g., read-write file, RWF) used in the course of it.

Figures 5 and 6 show the variation trends of both CPU and RWF-size as a function of diamine lenght and dicationic form (isolated or hydrochloride), using the mPW1PW/6-31G* and

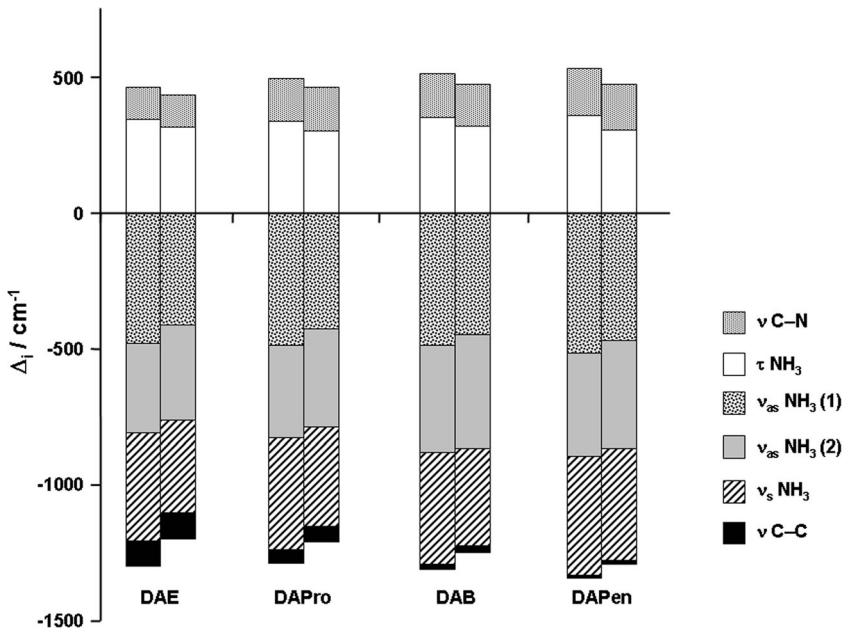

Fig. 4 Magnitude of the variation of the Δ_i-values (ω_i(amine−HCl)−ω_i(amine−H)) for some selected vibrational modes, as a function of diamine and theory level. In each set, left and right columns refer to the mPW1PW/6-31G* and ωB97XD/6-311++G(2d,2p) results, respectively

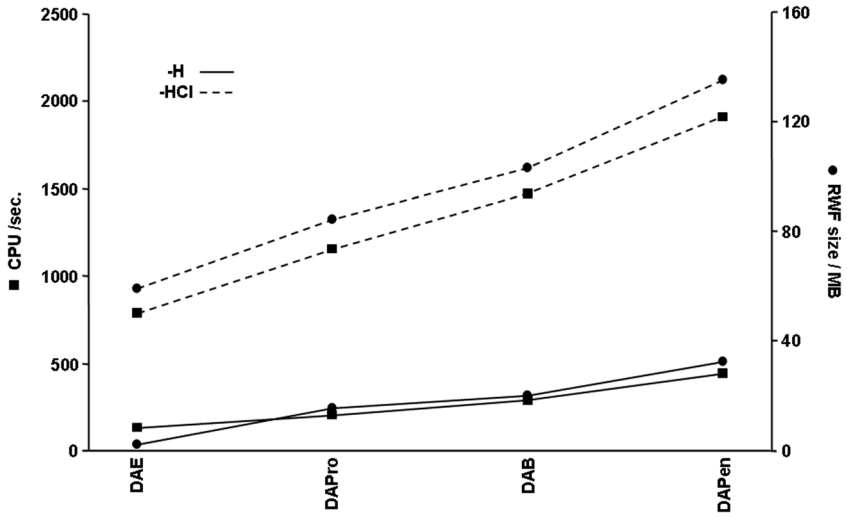

Fig. 5 Variation of CPU and RWF size as a function of diamine size and dicationic form (either isolated or hydrochloride species) at the mPW1PW/6-31G* theory level

ωB97XD/6-311++G(2d,2p) theory levels, respectively. With no surprise, increasing the diamine size leads to a considerable enhancement of computational demand (Figs. 5 and 6). Regardless of the theory level, a more drastic increase of both CPU and RWF-size is observed upon explicit consideration of the counterions. For the smallest diamine, for instance, changing from DAE-H to DAE-HCl, at the mPW1PW/6-31G* theory level, leads to a rise in CPU and RWF-size from 131 s and 2 MB to 782 s and 59 MB (597 and 2950 %, respectively). Increasing diamine size seems to reduce the growth rates of both computational parameters. However, this effect is only apparent and results from the fact that the explicit introduction of Cl^- ions in the calculation leads to a dramatic increase of the computational demand so that the effects resulting from amine size become comparatively less noticeable.

Regarding the effect of theory level (mPW1PW/6-31G* → ωB97XD/6-311++G(2d,2p)) it is verified that the increase observed for both CPU and RWF-size is even more pronounced than the ones due to the explicit account of the counterions (Fig. 5 vs. Fig. 6). As previously discussed, the decline of the growth rates associated to basis set upgrading is just apparent.

Nonetheless, the results presented herein clearly show that in order to extend the limits of applicability of quantum chemical calculations to gradually more complex systems, a coherent simplification of the theoretical approach is essential, as long as it does not compromise the results accuracy. This can be achieved either by reducing the calculation theory level and/or by simplifying the way of accounting for the effects of intermolecular interactions (e.g., interaction with counterions). In this context, the use of pre-defined scaling factors to correct vibrational frequency for the effects of the interactions with counterions represents a very attractive option. Furthermore, using this methodology associated within a low demanding theory level (as mPW1PW/6-31G*) makes it even more appealing.

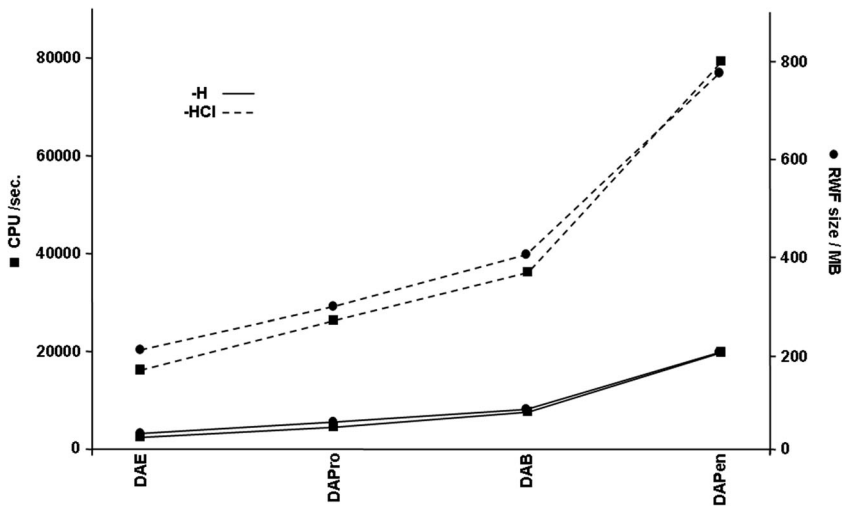

Fig. 6 Variation of CPU and RWF size as a function of diamine size and dicationic form (either isolated or hydrochloride species) at the ωB97XD/6-311++G(2d,2p) theory level

The correction factors

Table 1 comprises the group correction factors (ζ_g) determined for the four smaller α,ω-diamines, along with the corresponding averaging values (ζ_g^a), as a function of theory level. The sets of individual correction factors (ζ_i and ζ_i^a) are listed in Table S3 (Supplementary material) as a function of diamine and theory level. The similarity observed between the ζ_i-factors determined for certain categories of vibrational modes (Table S3) clearly suggests that the use of ζ_g-factors makes perfect sense. The similarity between correction factors extends to the equivalent ζ_i- and ζ_g-factors determined for the four diamines (Tables 1 and S3), and points out the possibility of using average factors (ζ_i^a and ζ_i^a). On the other hand, it also points to the possibility of restricting the number of distinct correction factors to seven or less (e.g., there is a great similarity between both ζ_i- and ζ_g-factors related to the δNH_3 and the distinct CH_2-related vibrational modes).

Finally, the effect of changing the theoretical level on the magnitude of the correction factors was assessed. As seen from Tables 1 and S3, simplifying the theory level from ωB97XD/6-311++G(2d,2p) to mPW1PW/6-31G* does not affect the magnitude of the correction factors. This observation suggests the possibility of transferability of the correction factors between different levels of theory. Supporting this idea, there are the correction factors determined based on calculations performed considering other theory levels. The gathered ζ_g^a scaling factors are given in Table 2 as a function of theory level.

Efficiency evaluation of the correction factors

In order to assess the relative efficiency of the four sets of correction factors (ζ_i, ζ_g, ζ_i^a or ζ_g^a), the RMSD and CV statistical parameters were determined for the corrections of the vibrational frequencies forecasted for the α,ω-diamines DAE, DAPro, DAB, and DAPen. The values are presented in Table 3, as a function of theory level and diamine, together with the corresponding values related to the uncorrected results. The general trends of improvement upon the different correction schemes apply equally to both theory levels.

Regardless of the correction factors set chosen, a great improvement is achieved for the implicit simulation of the interactions of the diamines with the counterions. A significant decrease of both RMSD and CV values relative to the uncorrected results is clear proof of that.

Unsurprisingly, the ranking of the sets of correction factors according to their efficiency to correct the vibrational frequencies calculated for isolated dicationic species to the effects of the interactions with counterions follows the order $\zeta_g^a < \zeta_g < \zeta_i^a < \zeta_i$, irrespective of diamine or theory level. Yet, the improvement achieved in using the set of ζ_g^a to account for the effects of the N–H···Cl interactions is obvious and opens up the possibility of using them to correct the vibrational frequencies predicted for the larger elements of the α,ω-diamine hydrochloride series.

Table 4 presents the RMSD and CV values obtained for the uncorrected and corrected (using the ζ_g^a given in Table 1) vibrational frequencies of the α,ω-diamines beyond DAHex. As stated previously, the calculations regarding these larger diamines were limited to the mPW1PW/6-31G* theory level. Such an option was based on the fact that this theory level provides a very good ratio between efficiency and computational demand, when compared with the higher level of theory ωB97XD/6-311++G(2d,2p).

The statistical results obtained clearly support the idea of the transferability of the ζ_g^a-factors determined using the smaller elements of the α,ω-diamines to correct the larger elements of the series. At first glance, the RMSD and CV values presented appear to suggest that the use of ζ_g^a-factors is more effective in the correction of the vibrational frequencies related to major elements of the series (which were not considered in their determination) than in the case of DAE, DAPro, DAB, and DAPen diamine (Table 3 vs. Table 4). This improvement is, however, apparent and it is also observed for the uncorrected results. A question thus arises regarding the reasons behind this apparent improvement.

Table 5 presents the RMSD and CV values determined for the entire α,ω-diamines series (both uncorrected and corrected vibrational frequencies, using the set of ζ_g^a-factors) considering all vibrational modes but the CH_2-related ones (δCH_2, ωCH_2, tCH_2 and ρCH_2). Recall that LAM modes and TAM are not considered for the reasons stated above.

Comparison of the RMSD and CV values presented in Table 5 with those listed in Tables 3 and 4 proves that the initially suggested improvement of the correction process with increase of diamine size is indeed illusory. The apparent improvement is a direct result of the dampening effect set up by the increase in the number of vibrational modes that are little, if at all, affected by the establishment of the N–H···Cl interactions. When this effect is circumvented by not considering the CH_2-related vibrational modes, two effects are noted. Firstly, the RMSD and CV values become less affected by the size of the diamine, becoming uniform throughout the whole α,ω-diamine series. Secondly, it becomes evident that the real improvement achieved by applying the correction ζ_g^a-factors is ultimately greater than that highlighted in Tables 2 and 3. In fact, removing CH_2-related vibrational modes from the calculation of the RMSD and CV values leads to an increase of the respective average values of those parameters from 155 cm^{-1} and 8.6 % to 237 cm^{-1} and 14.3 %, when the **UC** results are regarded, and from 24 cm^{-1} and 1.3 % to 31 cm^{-1} and 1.9 %, respectively, when the corrected vibrational frequencies are considered (Tables 2 and 3 vs. Table 4). In short, the worsening observed in the RMSD and CV values

Table 2 Average group correction factors (ζ_g^a) for an additional set of theory levels

Theory level	Vibrational modes [(a)]						
	ν NH_3	δ NH_3	ρ NH_3	τ NH_3	CH_2 [(b)]	ν C–C	ν C–N
mPW1PW/6-31G**	0.87	1.01	1.07	2.50	1.00	0.98	1.17
mPW1PW/6-31++G**	0.88	1.01	1.06	2.52	1.00	0.98	1.17
mPW1PW/aug-cc-pVDZ	0.88	1.01	1.06	2.53	1.00	0.98	1.17
mPW1PW/6-311++G(2d,2p)	0.88	1.01	1.06	2.50	1.00	0.97	1.16
B3LYP/6-31G*	0.88	1.01	1.08	2.45	1.00	1.00	1.15
B3LYP/6-31G**	0.87	1.01	1.07	2.48	1.00	0.97	1.17
B3LYP/6-31++G**	0.89	1.01	1.06	2.38	1.00	0.96	1.16
B3LYP/aug-cc-pVDZ	0.89	1.01	1.07	2.48	1.00	0.96	1.17
B3LYP/6-311++G(2d,2p)	0.88	1.01	1.07	2.51	1.00	0.96	1.16
M062X/6-31G*	0.90	1.01	1.06	2.38	1.00	0.98	1.17
M062X/6-31G**	0.89	1.01	1.06	2.34	1.00	0.98	1.17
M062X/6-31++G**	0.90	1.01	1.06	2.22	1.00	0.97	1.17
M062X/aug-cc-pVDZ	0.90	1.02	1.06	2.30	1.00	0.98	1.17
M062X/6-311++G(2d,2p)	0.90	1.01	1.06	2.26	1.00	0.97	1.16
X3LYP/6-31G*	0.88	1.01	1.07	2.48	1.00	0.98	1.17
X3LYP/6-31G**	0.87	1.01	1.07	2.48	1.00	0.98	1.17
X3LYP/6-31++G**	0.88	1.01	1.07	2.41	1.00	0.98	1.16
X3LYP/aug-cc-pVDZ	0.89	1.02	1.07	2.46	1.00	0.98	1.16
X3LYP/6-311++G(2d,2p)	0.88	1.01	1.07	2.42	1.00	0.98	1.16
LC-wPBE/6-31G*	0.89	1.02	1.06	2.47	1.00	0.98	1.17
LC-wPBE/6-31G**	0.89	1.02	1.06	2.48	1.00	0.98	1.17
LC-wPBE/6-31++G**	0.89	1.02	1.06	2.41	1.00	0.98	1.17
LC-wPBE/aug-cc-pVDZ	0.89	1.02	1.06	2.45	1.00	0.98	1.17
LC-wPBE/6-311++G(2d,2p)	0.89	1.02	1.06	2.44	1.00	0.98	1.17
ωB97XD/6-31G*	0.89	1.01	1.06	2.34	1.00	0.98	1.17
ωB97XD/6-31G**	0.88	1.01	1.07	2.36	1.00	0.98	1.17
ωB97XD/6-31++G**	0.89	1.01	1.06	2.26	1.00	0.97	1.17
ωB97XD/aug-cc-pVDZ	0.89	1.01	1.06	2.36	1.00	0.98	1.17
MP2/6-31G*	0.91	1.02	1.07	2.50	1.00	0.98	1.17
MP2/6-31G**	0.96	1.03	1.08	2.63	1.00	0.98	1.16

(a) ν=stretching; δ=deformation; t=twisting; ρ=rocking; ω=wagging; τ=torsion

(b) all CH_2-related modes (ν CH_2, δ CH_2, ω CH_2, t CH_2, and ρ CH_2)

is considerably more pronounced when considering the uncorrected results than when considering the corrected.

To finalize, similar variation trends of the RMSD and CV values were observed when the forecasts with other theory levels (Table 2) tested were regarded (results not shown).

Reliability evaluation

The significant deviations envisaged for some of the diamine vibrational modes upon the establishment of the N–H···Cl contacts suggest that using the theoretical predictions of isolated cationic diamine to assign the vibrational spectra of the respective salts may lead to relevant assignment flaws. For instance, the either explicit or implicit accounting of the N–H···Cl contacts promotes a significant downward shifting of the frequencies calculated for the νNH_3 to such an extent that they are clearly shifted to the spectral region typically associated to the νCH_2 vibrational modes or even to a region below that. Conversely, τNH_3 vibrations are diverted upward from the spectral region typically ascribed to the skeletal LAM and TAM vibrational modes to a spectral region just below the one ascribed to the ρCH_2 vibrations.

The results presented above clearly support the relevance of the two main issues evaluated. First, the use of correction factors to adjust the vibrational frequencies of dicationic amines for the effects of the intermolecular interactions constitutes an efficient way of bypassing the computational

Table 3 RMSD (cm^{-1}) and CV (%) values[(a)] obtained for the corrected vibrational frequencies predicted within the mPW1PW/6-31G* and ωB97XD/6-311++G(2d,2p) theory levels for DAE, DAPro, DAB, and DAPen

α,ω-diamine	UC [(b)]		C_i [(b,c)]		C_g [(b,d)]		C_i^a [(b,c)]		C_g^a [(b,d)]	
	RMSD	CV	RMSD	CV	RMSD	CV	RMSD	CV	RMSD	CV
mPW1PW/6-31G*										
DAE	199	10.8	6	0.3	31	1.7	19	1.0	35	1.9
DAPro	184	10.1	6	0.3	28	1.5	13	0.7	28	1.5
DAB	175	9.7	5	0.3	22	1.2	12	0.6	22	1.2
DAPen	169	9.4	6	0.3	25	1.4	15	0.8	27	1.5
ωB97XD/6-311++G(2d,2p)										
DAE	181	9.9	5	0.3	26	1.4	24	1.3	30	1.6
DAPro	170	9.4	7	0.4	21	1.2	16	0.9	22	1.2
DAB	169	9.3	8	0.5	18	1.0	12	0.7	22	1.2
DAPen	160	8.9	6	0.3	23	1.3	15	0.8	27	1.5

(a) The RMSD and CV values obtained considering the distinct correction schemes are compared with each other and with the corresponding non-corrected results (UC)

(b) UC=uncorrected; C_i and C_g stand for correction schemes using individual (ζ_i) and group (ζ_g) correction factors, respectively; superscript **a** stands for averaged values (see text)

(c) ζ_i and ζ_i^a taken from Table S3

(d) ζ_g and ζ_g^a taken from Table 1

demands associated with the explicit consideration of the counterions. Second, the simple mPW1PW/6-31G* theory level is once again confirmed as suitable for predicting the vibrational frequencies of aliphatic amines. The question that now arises concerns the reliability of the methodology to reproduce the experimental information available.

Starting with the νNH_3, the mPW1PW/6-31G* calculations on DAE-H predict these vibrational modes around 3480 ($\nu_{as}NH_3$), 3466 ($\nu_{as}NH_3$), and 3389 cm^{-1} ($\nu_{as}NH_3$) (Table S1), yielding RMSD and CV values of 596 and 20.9 %, respectively, when compared to the experimental values [26]. Applying the correction methodology proposed (using a ζ_g^a-factor of 0.88; Table 1) and afterward the scaling factor proposed by Merrick et al. [37] (λ=0.9499), the νNH_3 of DAE-H would be shifted to 2909, 2897, and 2815 cm^{-1}, respectively. These values are clearly closer to the experimentally ascribed values for the νNH_3 of DAE-HCl [26] (RMSD and CV values of 38 and 1.3 %, respectively). A similar

Table 4 RMSD (cm^{-1}) and CV (%) values obtained for the corrected vibrational frequencies predicted within the mPW1PW/6-31G* theory level for the six larger elements of the α,ω-diamine series (which were not used in the determination of the correction factors)

α,ω-diamine	UC [(a)]		C_g^a [(a)]	
	RMSD	CV	RMSD	CV
DAHex	151	8.4	19	1.1
DAHep	147	8.2	23	1.3
DAO	139	7.7	22	1.2
DAN	134	7.5	22	1.3
DADec	129	7.2	21	1.2
DADod	120	6.7	20	1.1

(a) UC=uncorrected; C_g^a stands for correction scheme using average group correction factors (Table 1)

Table 5 RMSD (cm^{-1}) and CV (%) values[(a)] obtained for the corrected vibrational frequencies predicted within the mPW1PW/6-31G* theory level for the whole α,ω-diamine series

α,ω-diamine	UC[(b)]		C_g^a [(b,c)]	
	RMSD	CV	RMSD	CV
DAE	248	14.0	41	2.3
DAPro	248	14.2	35	2.0
DAB	250	14.6	28	1.6
DAPen	253	15.0	35	2.1
DAHex	236	14.2	24	1.5
DAHep	236	14.4	28	1.7
DAO	230	14.2	29	1.8
DAN	228	14.3	30	1.9
DADec	225	14.2	29	1.8
DADod	217	14.1	30	1.9

(a)The CH_2-related modes are excluded from the RMSD and CV determination

(b) UC=uncorrected; C_g^a stand for correction using average group correction factors (see text)

(c) Using the correction factors presented in Table 1

observation can be drawn for the νNH_3 of DAB-HCl. The νNH_3 experimental values for DAB-HCl are around 2789, 3036, and 3073 cm^{-1} [33]. Applying the same correction-scaling methodology to the νNH_3 predicted for DAB-H clearly approaches the forecasted frequencies to the experimentally observed values — from 3512, 3504, and 3416 cm^{-1} (Table S1; RMSD and CV values are 518 and 17.5 %, respectively) to 2936, 2929, and 2855 cm^{-1} (RMSD and CV values are 108 and 3.6 %, respectively).

Regarding the two τNH_3, the experimental data on DAE-HCl [26], based on N-deuteration studies, ascribed one of these vibrational mode to a shoulder at *ca.* 469 cm^{-1}. Considering the DAE-H species, the mPW1PW/6-31G* (and all other theory levels tested) calculations predicted those modes to occur around 230–250 cm^{-1} (Table S1), far away from the experimental value. If the correction-scaling methodology proposed is applied, the deviation from the experimental value is clearly reduced, with the τNH_3 being predicted 596 and 528 cm^{-1}.

Conclusions

Amines are biologically relevant compounds being found ubiquitously in living organisms. At physiological pH they are found in their active, cationic form, interacting via electrostatic forces with other cellular components. Although the computational study of their unprotonated, isolated form, can be relatively straightforward, it can also be rather misleading as strong intermolecular interactions are not taken into account. The aim of the present work was to: (i) investigate by quantum mechanics the deviations encountered relative to the experimental data when considering or not the effect of the counterions on the prediction of the vibrational profile of diamines, (ii) find a set of correction factors that enabled a better estimate of the vibrational parameters without the need of considering the counterions explicitly on the calculation, (iii) test the transferability of the sets of correction factors to other diamines, and (iv) obtain these correction factors at the lowest computational cost possible while keeping a high efficiency. The systems used to obtain the sets of correction factors were the four smallest elements of the α,ω-diamines series (DAE, DAPro, DAB, and DAPen) which were computed at different theory levels. The methods were compared as to their proficiency on predicting the experimental data as well as to their computational demand.

It was found that there are non-negligible intermolecular effects occurring in the cationic species that must be considered when performing quantum mechanics calculations on these types of molecules. All vibrational modes are affected even if not equally, but as expected the most affected vibrational modes are the ones directly involved in the intermolecular interactions. Interestingly the sensitivity of the νC-C stretching mode becomes gradually lower as the carbon chain size increases most probably due to the loss of the coupling effect between terminal NH_3^+ groups.

Overall, the results suggest that the reliability of the effects that are anticipated for the vibrational frequencies of DAE, DAPro, DAB, and DAPen due to explicit accounting of the N–H···Cl interactions is not compromised by theoretical level simplification. Actually, the increase on diamine size (carbon skeletal increase) lead to a considerable increase of the computational requirements, increase in CPU and RWF-size, especially upon explicit accounting for the counterions. Therefore, the simplification of the theory level can be regarded as an advantage approach while maintaining high accuracy.

The analysis allowed the establishment of sets of group correction factors (ζ_g) and corresponding averaging values (ζ_g^a), for each theory level and for each of the four smaller α, ω-diamines studied. Theory level simplification from ωB97XD/6-311++G(2d,2p) to mPW1PW/6-31G* did not affect the magnitude of the correction factors. This suggests that transferability of the vibrational frequency correction factors is not only for different diamines but also between different levels of theory, their use being the best choice to account for the effects of the N–H···Cl interactions.

In summary, the analysis performed for the νNH_3 and τNH_3 modes clearly shows that the methodology proposed in this study is effective in predicting the vibrational frequency of the hydrochloride α,ω-diamine series. Its application allows predicting quite well the frequencies of those modes without the explicit consideration of the counterions. Moreover, the efficiency of the methodology is not compromised by the use of a simplified level of theory such as mPW1PW/6-31G *.

Acknowledgments The authors acknowledge financial support from the Portuguese Foundation for Science and Technology — Unidade de Química-Física Molecular (UID/Multi/00070/2013). Acknowledgements are also due to Laboratório Associado CICECO, University of Aveiro, Portugal, for the free access to computational facilities.

References

1. Hoet PHM, Nemery B (2000) Polyamines in the lung: polyamine uptake and polyamine-linked pathological or toxicological conditions. Am J Physiol Lung Cell Mol Physiol 278:L417–L433
2. Kusano T, Berberich T, Tateda C, Takahashi Y (2008) Polyamines: essential factors for growth and survival. Planta 228:367–381
3. Coburn RF (2009) Polyamine effects on cell function: possible central role of plasma membrane PI(4,5)P-2. J Cell Physiol 221: 544–551
4. Wallace HM (2009) In: Essays in essays in biochemistry, vol 46: the polyamines: small molecules in the omics era, vol. 46, Portland, London, pp 1–9.
5. Persson L (2009) In: essays in biochemistry, vol 46: the polyamines: small molecules in the omics era, vol. 46, Portland, London, pp 11–24

6. Handa AK, Mattoo AK (2010) Differential and functional interactions emphasize the multiple roles of polyamines in plants. Plant Physiol Biochem 48:540–546
7. Minarini A, Milelli A, Tumiatti V, Rosini M, Bolognesi ML, Melchiorre C (2010) Synthetic polyamines: an overview of their multiple biological activities. Amino Acids 38:383–392
8. Agostinelli E (2010) Polyamines in biological systems. Amino Acids 38:351–352
9. Huo Q-W, Li D-F, Long C (2012) PARP1 and atherosclerosis. Prog Biochem Biophys 39:423–428
10. Zhao T, Goh KJ, Ng HH, Vardy LA (2012) A role for polyamine regulators in ESC self-renewal. Cell Cycle 11:4517–4523
11. Iacomino G, Picariello G, D'Agostino L (2012) DNA and nuclear aggregates of polyamines. Biochim Biophys Acta Mol Cell Res 1823:1745–1755
12. Rajeeve V, Pearce W, Cascante M, Vanhaesebroeck B, Cutillas PR (2013) Polyamine production is downstream and upstream of oncogenic PI3K signalling and contributes to tumour cell growth. Biochem J 450:619–628
13. Decroos C, Bowman CM, Christianson DW (2013) Synthesis and evaluation of N-8-acetylspermidine analogues as inhibitors of bacterial acetylpolyamine amidohydrolase. Bioorg Med Chem 21: 4530–4540
14. Li C, Ma C, Xu P, Gao Y, Zhang J, Qiao R, Zhao Y (2013) Effective and reversible DNA condensation induced by a simple cyclic/rigid polyamine containing carbonyl moiety. J Phys Chem B 117:7857–7867
15. Minarini A, Milelli A, Tumiatti V, Rosini M, Lenzi M, Ferruzzi L, Turrini E, Hrelia P, Sestili P, Calcabrini C, Fimognari C (2013) Exploiting RNA as a new biomolecular target for synthetic polyamines. Gene 524:232–240
16. Wang S-Y, Lee AY-L, Lai Y-H, Chen JJW, Wu W-L, Yuann J-MP SW-L, Chuang S-M, Hou M-H (2012) Spermine attenuates the action of the DNA intercalator, actinomycin D, on DNA binding and the inhibition of transcription and DNA replication. PLoS One 7:e47101
17. Fiuza SM, Amado AM, Oliveira PJ, Sardão VA, Batista de Carvalho LAE, Marques MPM (2006) Pt(II) vs Pd(II) polyamine complexes as new anticancer drugs: a structure-activity study. Lett Drug Des Disc 3:149–151
18. Tummala R, Diegelman P, Fiuza SM, Batista de Carvalho LAE, Marques MPM, Kramer DL, Clark K, Vujcic S, Porter CW, Pendyala L (2010) Characterization of Pt-, Pd-spermine complexes for their effect on polyamine pathway and cisplatin resistance in A2780 ovarian carcinoma cells. Oncol Rep 24:15–24
19. Shingu T, Chumbalkar VC, Gwak H-S, Fujiwara K, Kondo S, Farrell NP, Bogler O (2010) The polynuclear platinum BBR3610 induces G2/M arrest and autophagy early and apoptosis late in glioma cells. Neuro-Oncology 12:1269–1277
20. McGregor TD, Hegmans A, Kasparkova J, Neplechova K, Novakova O, Penazova H, Vrana O, Brabec V, Farrell N (2002) A comparison of DNA binding profiles of dinuclear platinum compounds with polyamine linkers and the trinuclear platinum phase II clinical agent BBR3464. J Biol Inorg Chem 7:397–404
21. Navarro-Ranninger C, Pérez JM, Zamora F, González VM, Masaguer JR, Alonso C (1993) Palladium(II) Compounds of putrescine and spermine — synthesis, characterization, and DNA-binding and antitumor properties. J Inorg Biochem 52:37–49
22. Fiuza SM, Holy J, Batista de Carvalho LAE, Marques MPM (2011) Biologic activity of a dinuclear Pd(II)-spermine complex toward human breast cancer. Chem Biol Drug Des 77:477–488
23. Soares AS, Fiuza SM, Goncalves MJ, Batista de Carvalho LAE, Paula M, Marques MPM, Urbano AM (2007) Effect of the metal center on the antitumor activity of the analogous dinuclear spermine chelates (PdCl2)(2)(spermine) and(PtCl2)(2)(spermine). Lett Drug Des Disc 4:460–463
24. Amado AM, Fiuza SM, Batista de Carvalho LAE, Ribeiro-Claro PJA (2013) On the relevance of considering the intermolecular interactions on the prediction of the vibrational spectra of isopropylamine. J Chem Article ID 682514
25. Amado AM, Fiuza SM, Marques MPM, Batista de Carvalho LAE (2007) Conformational and vibrational study of platinum(II) anticancer drugs: cis-diamminedichloroplatinum(II) as a case study. J Chem Phys 127:185104
26. Amado AM, Otero JC, Marques MPM, Batista de Carvalho LAE (2004) Spectroscopic and theoretical studies on solid 1,2-ethylenediamine dihydrochloride salt. ChemPhysChem 5:1837–1847
27. Batista de Carvalho LAE, Marques MPM, Tomkinson J (2006) Transverse acoustic modes of biogenic and α, ω-polyamines: a study by inelastic neutron scattering and Raman spectroscopies coupled to DFT calculations. J Phys Chem A 110:12947–12954
28. Fiuza SM, Amado AM, dos Santos HF, Marques MPM, Batista de Carvalho LAE (2010) Conformational and vibrational study of cis-diamminedichloropalladium(II). Phys Chem Chem Phys 12: 14309–14321
29. Silva TM, Andersson S, Sukumaran SK, Marques MP, Persson L, Oredsson S (2013) Norspermidine and novel Pd(II) and Pt(II) polynuclear complexes of norspermidine as potential antineoplastic agents against breast cancer. Plos One 8
30. Marques MPM, Gianolio D, Cibin G, Tomkinson J, Parker SF, Valero R, Pedro Lopes R, Batista de Carvalho LAE (2015) A molecular view of cisplatin's mode of action: interplay with DNA bases and acquired resistance. Phys Chem Chem Phys 17:5155–5171
31. Marques MPM, Valero R, Parker SF, Tomkinson J, Batista de Carvalho LAE (2013) Polymorphism in cisplatin anticancer drug. J Phys Chem B 117:6421–6429
32. Lopes RP, Valero R, Tomkinson J, Marques MPM, Batista de Carvalho LAE (2013) Applying vibrational spectroscopy to the study of nucleobases — adenine as a case-study. New J Chem 37: 2691–2699
33. Amorim da Costa AM, Marques MPM, Batista de Carvalho LAE (2003) Raman spectra of putrescine, spermidine and spermine polyamines and their N-deuterated and N-ionized derivatives. J Raman Spectrosc 34:357–366
34. Fiuza SM, Amado AM, Parker SF, Marques MPM, Batista de Carvalho LAE (2015) Conformational insights and vibrational study of a promising anticancer agent: the role of the ligand in Pd(II)-amine complexes. New J Chem 39:6274–6283
35. Irikura KK, Johnson RD, Kacker RN (2005) Uncertainties in scaling factors for ab initio vibrational frequencies. J Phys Chem A 109: 8430–8437
36. Andersson MP, Uvdal P (2005) New scale factors for harmonic vibrational frequencies using the B3LYP density functional method with the triple-ζ basis set 6–311+G(d, p). J Phys Chem A 109: 2937–2941
37. Merrick JP, Moran D, Radom L (2007) An evaluation of harmonic vibrational frequency scale factors. J Phys Chem A 111:11683–11700
38. Frisch MJ, Trucks GW, Schlegel HB, Scuseria GE, Robb MA, Cheeseman JR, Scalmani G, Barone V, Mennucci B, Petersson GA, Nakatsuji H, Caricato M, Li X, Hratchian HP, Izmaylov AF, Bloino J, Zheng G, Sonnenberg JL, Hada M, Ehara M, Toyota K, Fukuda R, Hasegawa J, Ishida M, Nakajima T, Honda Y, Kitao O, Nakai H, Vreven T, Montgomery JA Jr, Peralta JE, Ogliaro F, Bearpark M, Heyd JJ, Brothers E, Kudin KN, Staroverov VN, Kobayashi R, Normand J, Raghavachari K, Rendell A, Burant JC, Iyengar SS, Tomasi J, Cossi M, Rega N, Millam JM, Klene M, Knox JE, Cross JB, Bakken V, Adamo C, Jaramillo J, Gomperts R, Stratmann RE, Yazyev O, Austin AJ, Cammi R, Pomelli C, Ochterski JW, Martin RL, Morokuma K, Zakrzewski VG, Voth

GA, Salvador P, Dannenberg JJ, Dapprich S, Daniels AD, Farkas O, Foresman JB, Ortiz JV, Cioslowski J, Fox DJ (2009) Gaussian 09, Revision A.02. Gaussian Inc, Wallingford

39. Varadwaj A, Varadwaj PR, Jin B-Y (2015) Fluorines in tetrafluoromethane as halogen bond donors: revisiting address the nature of the fluorine's sigma(hole). Int J Quantum Chem 115:453–470
40. Liu Y, Zhao J, Li F, Chen Z (2013) Appropriate description of intermolecular interactions in the methane hydrates: an assessment of DFT methods. J Comput Chem 34:121–131
41. Sun T, Wang Y-B (2011) Calculation of the binding energies of different types of hydrogen bonds using gga density functional and its long-range, empirical dispersion correction methods. Acta Phys -Chim Sin 27:2553–2558
42. Thanthiriwatte KS, Hohenstein EG, Burns LA, Sherrill CD (2011) Assessment of the performance of DFT and DFT-D methods for describing distance dependence of hydrogen-bonded interactions. J Chem Theory Comput 7:88–96
43. Arderne C (2013) Pentane-1,5-diaminium dibromide. Acta Crystallogr Sect C Cryst Struct Commun 69:526–528
44. Ashida T, Hirokawa S (1963) The crystal structure of ethylenediammonium chloride. Bull Chem Soc Jpn 36:704–707
45. Ashida T, Hirokawa S (1963) The crystal structure of tetramethylenediammonium chloride. Bull Chem Soc Jpn 36: 1086–1091
46. Ashida T, Hirokawa S (1963) Crystal structures of ethylenediammonium chloride and tetramethylenediammonium chloride. Acta Crystallogr 16:841–842
47. Brisson J, Brisse F (1982) New refinement of the crystal-structure of 1,3-diaminopropane dihydrochloride. J Crystallogr Spectrosc Res 12:39–43
48. Bujak M, Sikorska L, Zaleski J (2000) Structure and phase transitions in ethylenediammonium dichloride and its salts with antimony trichloride. Zeitschrift Fur Anorganische Und Allgemeine Chemie 626:2535–2542
49. Chandrasekhar K, Pattabhi V (1980) Redetermination of the structure of putrescine dihydrochloride. Acta Crystallogr Sect B Struct Sci 36:2486–2488
50. Gabro M, Lalancette RA, Bernal I (2009) Ethylenediammonium dichloride. Acta Crystallogr Sect E Struct Rep Online 65:O1352
51. Pospieszna-Markiewicz I, Radecka-Paryzek W, Kubicki M (2006) Cadaverinium dichloride: a case of centro-non-centrosymmetric ambiguity. Acta Crystallogr Sect C Cryst Struct Commun 62: O399–O401
52. Søtofte I (1976) Crystal-Structure of Ethylenediammonium Bromide. Acta Chem Scand Ser A Phys Inorg Chem 30:309–311
53. van Blerk C, Kruger GJ (2007) Butane-1,4-diammonium dibromide. Acta Crystallogr Sect E Struct Rep Online 63:O342–O344
54. Dennington R, Keith T, Millam J (2009) GaussView, Version 5. Gaussian Inc, Shawnee Mission
55. Marques MPM, Batista de Carvalho LAE, Tomkinson J (2002) Study of biogenic and α, ω-polyamines by combined inelastic neutron scattering and Raman spectroscopies and by ab initio molecular orbital calculations. J Phys Chem A 106:2473–2482
56. Tomkinson J, Parker SF, Braden DA, Hudson BS (2002) Inelastic neutron scattering spectra of the transverse acoustic modes of the normal alkanes. Phys Chem Chem Phys 4:716–721